

## ORIGINAL ARTICLE

# Surface Optimization of nano porous *Ceiba pentandra* hull carbon for the removal of Methylene blue from Aqueous Solution: Kinetics and Isotherms

R.Subha\*<sup>1</sup> and D.Anitha<sup>2</sup>

Assistant Professor, Department of Chemistry, Karpagam Institute of Technology, Coimbatore, India

Email: subhavijay1@gmail.com

### ABSTRACT

Activated carbon prepared from *Ceiba pentandra* hull using  $ZnCl_2$  (ZnCPC) was investigated to find the feasibility and its application for removal of methylene blue in aqueous solution through adsorption process. Batch mode kinetics and isotherm studies were carried out to evaluate the effects of contact time, initial concentration, adsorbent dose, pH, and temperature. Lagergren, Second order, and Banghams plots were used to fit the experimental data. Langmuir, Freundlich, D-R and Temkin isotherm models have been employed to analyse the adsorption equilibrium data. The Langmuir adsorption capacity  $Q_0$  was found to be  $134.5 \text{ mg g}^{-1}$  of the adsorbent. pH effect and desorption studies showed that physisorption mechanism was involved in the adsorption process. Removal efficiency of methylene blue from synthetic wastewater was also tested.

**Key words:** *Ceiba pentandra*, Activated carbon, Methylene blue, Kinetics, Isotherms, pH effect.

Received 23.04.2017 Accepted 19.07.2017

© 2017 AELS, INDIA

### Introduction

Every year a considerable volume of dye-laden effluents from manufacturing industries infiltrates the water systems of many countries around the world [1]. The presence of dyes in effluents even at low concentration produce a number of toxic products via hydrolysis, chemical method is very harmful to human beings. Because of their low cost and potential applications in industries, more than ten thousand new dyes are introduced annually [2]. Methylene blue (MB), a cationic dye is most commonly used as the coloring agent for cotton, wool and silk. It is also used as a staining agent to make certain body fluids and view tissues earlier during surgery and diagnostic examinations [3]. Consequently, MB readily adsorbs onto a wide variety of adsorbents from industrial waste [4] to advanced materials [5,6] including minerals [7]. The medical application of MB include the treatment of methaemoglobinemia and cyanide poisoning. In spite of several applications, this dye has a number of negative impacts on human beings and animals; such as irritation of mouth, throat, oesophagus and stomach with symptoms of nausea, abdominal discomfort, vomiting and diarrhea. Skin contact may cause mechanical irritation resulting in redness and itching [3].

Various treatment processes such as adsorption [8,9,10], membrane process [11], coagulation-flocculation [12] and electrochemical oxidation [13] have been used for the removal of dye from wastewater. Due to high efficiency, cost effectiveness and simple operation, adsorption of contaminants from wastewater has received a great deal of attention [14]. The adsorption behaviour of MB onto  $TiO_2$  nanoparticle containing hydrogel nanocomposite (HNC) of polyacrylamide-grated gum ghatti was highly influenced by hydrophobic interaction [1].

Patra et al found an efficient polysaccharide agar based adsorbent by modifying mono metallic/bimetallic nanoparticle (Fe, Cu, Pd, Fe/Cu and Fe/Pd) to remove methylene blue. The maximum adsorption capacity of agar Fe/Pd nanoparticle was found to be  $875 \text{ mg/g}$  respectively. The adsorption studies suggest that bimetallic nanoparticle have more efficiency in comparison to monometallic system [15]. Various adsorbents such as agar based bimetallic nanoparticles [15],  $Fe_3O_4$ /activated montmorillonite composite [2], clay soil [16], citrus limetta peel waste [3], municipal sewage sludge and tea waste [17], oil palm leaves [18], gum ghatti/ $TiO_2$  nanoparticles [1], Raspberry like  $TiO_2$ @yeast microphores [19], Biochar from pine wood, pig manure and cardboard [20], k-carrageenan- $Fe_3O_4$  nanoparticles [21],  $^{YY}Fe_2O_3/SiO_2$

nanocomposite [22], Zirconium selenotunstoposphate [23] for removal of Methylene blue has been reported. However they are not cost effective.

*Ceiba pentandra* tree is widely distributed in deciduous forests of western and eastern India. All the plant parts like root, bark gum, leaf and cotton from fruit are widely used. *Ceiba pentandra* hull is non toxic, biodegradable, light weight agricultural waste of less importance. Activation of ceiba with  $ZnCl_2$  generates more interspaces between carbon layers leading to more micro porosity and more surface area compared to the carbon prepared in the absence of  $ZnCl_2$ . The increase in porosity with  $ZnCl_2$  activation suggests that the porosity created by this reactant is due to the spaces left by  $ZnCl_2$  after the corresponding washing.  $ZnCl_2$  activation causes electrolytic action termed as "swelling" in the molecular structure of cellulose, which leads to the breaking of lateral bonds in the cellulose molecules resulting in increased inter- and intra- voids.  $ZnCl_2$  promotes the development of porous structure of the activated carbon because of the formation of small elementary crystallites [24].

In this study, the focus is to evaluate the potential of  $ZnCl_2$  activated ceiba pentandra hull carbon for adsorption of methylene blue from aqueous solution. Adsorption dynamics, isotherm, effect of pH, adsorbent dose and temperature were studied. Application to treatment of synthetic wastewater containing methylene blue was also carried out.

## MATERIAL AND METHOD

*Ceiba pentandra* hull was collected from local industries. It was dried in sunlight for 5 h. The dried ceiba hull (200 g) was stirred in a boiling solution of anhydrous  $ZnCl_2$  (100 g in 1 liter of distilled water) for 1 h, then the remaining solution was drained off and dried at 60°C for 12 h. This material was packed in a steel container and placed inside another concentric steel container packed with sand. The whole set up was placed in a muffle furnace at 700°C and carbonization was done for 1 h. After cooling the excess zinc chloride present in the carbonized material was leached out by immersing in 1 M HCl solution for about 24 h in an oven at 80°C. Then the carbon was repeatedly washed with water to get rid of traces of HCl and  $ZnCl_2$ . This was ascertained by analyzing the wash water each time using silver nitrate. The carbonized material was sieved to 250 to 500  $\mu m$  size and characterized using physico-chemical methods and used for adsorption studies [25]. Experimental solutions of MB were prepared using analytical reagent grade obtained from Loba chemie, Mumbai. Synthetic waste waters containing MB of 20 and 60  $mgL^{-1}$  were prepared using analytical reagent grade salts, NaCl,  $CaCl_2$ ,  $Na_2CO_3$ ,  $NaHCO_3$  and  $Na_2SO_4$  and their composition: chloride (49.6  $mg L^{-1}$ ), sulfate (58  $mg L^{-1}$ ), calcium (20  $mg L^{-1}$ ), carbonate (10  $mg L^{-1}$ ) and sodium (59.6  $mg L^{-1}$ ) [26].

Batch mode adsorption studies were carried out by agitating 50 mg of CPC/ZnCPC with 50 ml of MB solution of desired concentration on a thermostated rotary shaker (ORBITEK, Chennai, India) at 200 rpm, 35°C and at an initial pH 2.0. At the end of adsorption, the solution and adsorbent were separated by centrifugation at 10,000 rpm for 20 min and the concentration of residual MB was determined spectrophotometrically using UV-Visible spectrophotometer at 690 nm (Specord 200, Analytic Jena, Germany). Effect of contact time was studied by withdrawing samples at predetermined time intervals and then residual concentration was analyzed as before. Effect of pH was studied in the pH range 2.0 to 11.0 by adjusting the pH using 0.1 M HCl and 0.1 M NaOH solutions by means of a pH meter (Elico, Mode LI-107, Hyderabad, India). Effect of adsorbent dose was studied with different adsorbent doses (10-250 mg) for MB solutions (20-100  $mg L^{-1}$ ).

Effect of temperature on adsorption of MB was studied using 20-100  $mg L^{-1}$  concentration and 50 mg of the adsorbent at 35, 40, 50, 60 °C in a thermostated rotary shaker. The adsorbent (50 mg per 50 ml) that was used for the adsorption of 20-100  $mg L^{-1}$  of MB solution was separated from the solution by suction-filtration using Whatman filter paper and washed gently with water to remove any unadsorbed MB. Then the spent adsorbent was mixed with 50 ml of distilled water whose pH was adjusted to various values (2.0-11.0) and agitated at time intervals longer than the equilibrium time. Then the desorbed MB was estimated as before.

## RESULTS AND DISCUSSION

The physio-chemical characteristics of ZnCPC in comparison with the CPC is given in Tables 1. The ZnCPC has a higher surface area (786  $m^2 g^{-1}$ ) compared to the CPC (184  $m^2 g^{-1}$ ). Most of the surface (80%) and pore volume (72%) was made up by pores smaller than 2 nm in pore width, the so called micropores. The carbon has a sponge like structure, due to the very high value of the fractal dimension with 2.93. As the pore diameter is less than 2 nm, ZnCPC can be considered as nano porous carbon [25]. In the present study, SEM was used to assess morphological changes in the carbon surfaces following adsorption of the MB.  $ZnCl_2$  activated ceiba pentandra hull carbon before adsorption (250 X magnification) revealed voids with a large number of pores (Figure 1a). After adsorption the pores were filled by MB (Figure 1b). Coverage of the surface of the adsorbent due to adsorption of the adsorbate molecule presumably leading to

formation of a monolayer of the adsorbate molecule over the adsorbent surface is evident from the formation of white layer (molecular cloud) of uniform thickness and coverage (spread). The preparation of activated carbon from solid olive waste with 20% ZnCl<sub>2</sub> after mixing and subjected to vacuum drying with 500 times magnification reveals solid has different types of pores with different parameters and there was a scattering of salt particles on the surface of the activated carbon [27]. This was due to the presence of remaining zinc chloride or other metal compounds on the activated carbon. Some particles were even trapped into the pores and could possibly block the entry of pores to some extent [24].

#### **Effect of reaction time and kinetics**

The amount of MB adsorbed (mg g<sup>-1</sup>) increased with increase in agitation time and reached equilibrium. The equilibrium time was found to be 90, 120, 150, 160 and 180 min for 20, 40, 60, 80, 100 mg L<sup>-1</sup>, respectively. The amount of MB removed at equilibrium increased from 9.830 to 73.42 mg g<sup>-1</sup> with increase in MB concentration from 20 to 100 mg L<sup>-1</sup>. It shows that the adsorption at different concentrations was rapid in the initial stages and gradually decreased with the progress of adsorption until the equilibrium was reached.

#### **Adsorption kinetics**

Adsorption kinetic models correlate the adsorbate uptake rate with bulk concentration of the adsorbate. Kinetic data were fit into Lagergren [28], Second order [29] and Banghams pore diffusion [30] models.

The first order kinetic model is represented as:

$$\log(q_e - q) = \log q_e - k_1 t / 2.303 \quad (1)$$

where  $q_e$  and  $q$  are the amounts of MB adsorbed (mg g<sup>-1</sup>) at equilibrium and at time  $t$ , respectively, and  $k_1$  is the Lagergren rate constant of first order adsorption (min<sup>-1</sup>).

The second order kinetic model is expressed as:

$$t/q = 1/k_2 q_e^2 + t/q_e \quad (2)$$

where  $k_2$  is the rate constant of second order adsorption (g mg<sup>-1</sup> min<sup>-1</sup>).

The experimental  $q_e$  values were closer to the calculated  $q_e$  values obtained from the second order kinetic plots compared to those of the first order kinetic plots (Table 2). The correlation coefficients are closer to unity for second order kinetic model. Therefore, the adsorption kinetics can well be approximated more favorably by second order kinetic model for MB. Similar phenomenon has been observed in the adsorption of MB by NaOH activated chitosan flakes [31].

Bangham's equation was used to evaluate whether the adsorption is pore-diffusion controlled.

$$\log\{\log[C_0/(C_0 - qM)]\} = \log(K_0 M / 2.303V) + \alpha \log t \quad (3)$$

where  $C_0$  is initial concentration (mmolL<sup>-1</sup>),  $V$  is volume of the solution (ml),  $M$  is weight of the adsorbent (g dm<sup>-3</sup>),  $q_m$  is amount of adsorbate retained at time 't' (mmolg<sup>-1</sup>) and  $\alpha$ ,  $K_0$  are constants. The values of  $\alpha$  and  $K_0$  are given in Table 2. Plots of  $\log\{\log[C_0/(C_0 - q_m)]\}$  vs  $\log t$  ( $R^2 = 0.93$  to  $0.99$ ) were found to be linear for different concentrations at 35°C which confirms that the adsorption is pore-diffusion controlled.

Increase in adsorbent dose increased the removal of MB and quantitative removal occurred at 150, 200, 250, 300 and 400 mg per 50 ml adsorbent dose for 20, 40, 60, 80 and 100 mg L<sup>-1</sup> concentration of MB, respectively. Increase in adsorption with adsorbent dose is attributed to greater surface area and the availability of more adsorption sites.

#### **Adsorption isotherms**

The equilibrium adsorption isotherm is fundamentally very crucial in designing adsorption systems. In this study, adsorption of MB by ZnCPC was analyzed by well documented Langmuir (Eq.4) [32], Freundlich (Eq.5) [33], Dubinin-Radushkevich (Eq.6) [34] and Temkin (Eq.7) [35] isotherm models given below, respectively (Fig.2).

$$C_e/q_e = 1/Q_0 b + C_e/Q_0 \quad (4) \quad \log$$

$$q_e = \log k_f + 1/n \log C_e \quad (5)$$

$$\ln q_e = \ln q_m - \beta \epsilon^2 \quad (6)$$

$$q_e = B \ln A + B \ln C_e \quad (7)$$

where in Eq.4,  $C_e$  is the concentration of MB solution (mg L<sup>-1</sup>) at equilibrium,  $Q_0$  gives the theoretical monolayer adsorption capacity (mg g<sup>-1</sup>) and  $b$  is related to the energy of adsorption (mg L<sup>-1</sup>). In Eq.5,  $k_f$  and  $1/n$  are the constants that can be related to adsorption capacity and the intensity of adsorption respectively. In Eq.6,  $q_m$  is the theoretical saturation capacity (mol/g),  $\beta$  is a constant related to the mean free energy of adsorption per mole of the adsorbate (mol<sup>2</sup>/J<sup>2</sup>), and  $\epsilon$  is the Polanyi potential. In Eq. 7,  $A$  and  $B$  are constants.

Langmuir constants,  $Q_0$  and  $b$ , were calculated from the linear plot of  $C_e/q_e$  vs  $C_e$  and found to be 134.5 mg g<sup>-1</sup> and 0.9689 L mg<sup>-1</sup>, respectively. The adsorption capacity of cebia pentandra hull carbon (in the absence of ZnCl<sub>2</sub> activation) for MB was found to be negligible (0.012 mg L<sup>-1</sup>). Higher surface area and

higher pore volume of the ZnCPC are responsible for the good adsorption capacity of the carbon for MB. The Freundlich constants,  $k_f$  and  $n$  were evaluated from the linear plots of  $\log q_e$  vs  $\log C_e$  and found to be  $81.66 \text{ mg}^{1-1/n} \text{ L}^{1/n} \text{ g}^{-1}$  and 2.14, respectively. The value of  $n$  lies between 1 and 10 indicating favorable adsorption [36]. The D-R constants  $q_m$  and  $\beta$  were evaluated from the linear plots of  $\ln q_e$  vs  $\epsilon^2$  and found to be  $1596 \text{ mol g}^{-1}$  and  $3 \times 10^{-9} \text{ mol}^2 \text{ J}^{-2}$ , respectively. The constant  $\beta$  give an idea about the mean free energy  $E$  ( $\text{kJ mol}^{-1}$ ) of adsorption [34]. The value of  $E$  ( $12.9 \text{ kJ mol}^{-1}$ ) is between 8 and  $16 \text{ kJ mol}^{-1}$  which shows that the adsorption follows physisorption mechanism [37]. The Temkin isotherm constants  $A$  and  $B$  were found to be  $4.001 \text{ Lmg}^{-1}$  and  $10.6 \text{ mg g}^{-1}$ , respectively. Langmuir, Freundlich, D-R and Temkin constants for adsorption of MB by various adsorbents reported in literature are presented in Table 3. Taking into account the cost of other activated carbons and ZnCPC; it is obvious that ZnCPC is cost effective, because the raw material is an unwanted waste and does not have any commercial value.

Figure 2 presents different adsorption isotherms along with the experimental data. In order to compare the validity of isotherms, a normalized deviation,  $\Delta q(\%)$ , was calculated using the following equation [38]:

$$\Delta q(\%) = 100 \times \sqrt{\frac{\sum [(q_e^{\text{exp}} - q_e^{\text{cal}}) / q_e^{\text{exp}}]^2}{(n - 1)}} \quad (8)$$

where superscripts 'exp' and 'cal' are the experimental and calculated values, respectively, and 'n' is the number of measurements. From the results, it was found that values of  $\Delta q$  obtained from Langmuir [ $\Delta q(\%) = 3.7$ ], and Freundlich [ $\Delta q(\%) = 7.78$ ], were lower compared to D-R [ $\Delta q(\%) = 11.8$ ] and Temkin [ $\Delta q(\%) = 29.3$ ] adsorption isotherm models. It shows that the equilibrium data fit better with Langmuir and Freundlich isotherms over the entire range of concentrations compared to D-R and Temkin isotherms. Increase of temperature hardly increased the amount adsorbed at equilibrium,  $q_e$  (Table 2) which shows that temperature had no effect on adsorption.

#### Effect of pH

The effect of solution pH on the adsorption of MB using ZnCPC was studied in dye solution of different pH values. Initially, the removal decreased with increase in the solution pH (Fig.3). In the acidic medium, the positively charged amino groups of MB becomes protonated, therefore the excess of  $\text{H}^+$  ions on the surface competes with cationic dye for adsorption sites. This result in electrostatic repulsion between ZnCPC surface and dye. When the pH is greater than  $\text{zpc}$ , the concentration of  $\text{H}^+$  ion decreased in the solution and there exist competitive adsorption and repulsive interaction between MB and  $\text{H}^+$  ions increasing the adsorption amount. But in more basic medium (ie.>8.0), the hydroxyl ions may get interacted with positively charged dye molecule resulting in poor binding [15]

#### Batch mode desorption studies

Desorption studies helps to elucidate the mechanism of adsorption and recover the precious MB and adsorbent. As the desorbing pH was increased, the per cent desorption increased from 4.13% at pH 2.0 to 54 % at pH 6.0 and then decreased to 11.06 % at pH 11.0 for  $60 \text{ mg L}^{-1}$  (Fig. 3). This is due to the increased concentration of  $\text{OH}^-$  leading to electrostatic repulsion between positively charged MB dye and surface. Studies on both pH effect and desorption show that physisorption was involved for the removal of MB by ZnCPC.

#### Tests with synthetic wastewater

Effect of pH and adsorbent dose on the adsorption of MB from synthetic waste water is similar to pure MB solutions. Maximum removal of 83.9 and 75 %, respectively, was observed at pH 10.0 for the MB concentrations 20 and  $60 \text{ mg L}^{-1}$  in the wastewater compared to 89.1 and 79 % in pure MB solutions. Quantitative removal was observed at an adsorbent dose of 100 and  $300 \text{ mg}/50\text{ml}$  for the MB concentrations of 20 and  $60 \text{ mg L}^{-1}$ , respectively, in the waste water compared to 70 and  $250 \text{ mg}/50 \text{ ml}$  in pure MB solutions. Lower per cent removal in pH effect and higher adsorbent dose requirement in adsorbent dose effect for the removal of MB in wastewater are attributed to the presence of other competing components such as  $\text{Cl}^-$  and  $\text{SO}_4^{2-}$  in the waste water.

**Table 1: Physio-chemical characteristics of activated *Cebia pentandra* hull carbons**

Parameter	With $\text{ZnCl}_2$ activation	Without $\text{ZnCl}_2$ activation
Specific surface area ( $\text{m}^2 \text{ g}^{-1}$ )	786	184
Total pore volume ( $\text{cm}^3 \text{ g}^{-1}$ )	0.363	0.122
Micropore area ( $\text{m}^2 \text{ g}^{-1}$ )	284.0	89.3
Micropore volume ( $\text{cm}^3 \text{ g}^{-1}$ )	0.131	0.091
$\text{pH}_{\text{ZPC}}$	3.7	8.00
Conductivity (1% solution) ( $\text{mS}/\text{cm}$ )	0.18	2.30
Mechanical Moisture content (%)	9.0	5.88
Ash content (%)	4.21	8.00

Porosity (%)	89.1	75.1
Decolorizing power (mg g <sup>-1</sup> )	137.00	21.00
Iodine number (mg g <sup>-1</sup> )	210.04	101.52
Ion exchange capacity (meq g <sup>-1</sup> )	0.11	Nil
Zinc (%)	0.02	-
Zinc leached (%)	0.01	-
Ash analysis:		
Sodium (%)	5.1	0.14
Potassium (%)	1.2	0.18
Calcium (%)	0.78	0.22
Phosphorous (%)	0.01	0.01

**Table 2 :** Comparison of first order and second order adsorption rate constants and Banghams constants and calculated and experimental  $q_e$  values for different initial MB concentrations and for different temperatures

Parameter Concn (mgL <sup>-1</sup> )*	$q_e(\text{exp})$ mg g <sup>-1</sup>	First order Kinetics			Second order Kinetics			Banghams Model		
		$k_1(\text{min}^{-1})$	$q_e(\text{cal})$ (mg g <sup>-1</sup> )	$R^2$	$k_2$ (g mg min <sup>-1</sup> )	$q_e$ (cal) (mgg <sup>-1</sup> )	$R^2$	$k_0$	$\alpha$	$R^2$
20	9.83	0.039	7.71	0.99	0.0076	10.18	0.99	11.3	0.41	0.93
40	17.32	0.016	12.36	0.98	0.0035	17.86	0.99	19.7	0.34	0.99
60	35.16	0.021	21.33	0.98	0.0016	36.03	0.99	31.2	0.30	0.98
80	51.26	0.024	26.31	0.95	0.0013	51.77	0.99	42.1	0.32	0.97
100	73.42	0.028	52.32	0.98	0.0006	74.51	0.99	60.1	0.38	0.96
Temp °C+										
35	9.83	0.039	7.71	0.96	0.0076	10.18	0.99	11.3	0.41	0.93
40	9.81	0.041	7.42	0.93	0.0072	10.6	0.99	11.4	0.40	0.97
50	9.82	0.043	7.90	0.96	0.0075	10.12	0.99	11.5	0.39	0.95
60	9.83	0.044	7.16	0.98	0.0071	10.21	0.99	11.1	0.38	0.97

\*Conditions: Adsorbent dose, 50 mg/50 ml; pH 10.0; Temp. 35 °C.

+Conditions: Conc., 20 mg L<sup>-1</sup>; Adsorbent dose, 50 mg/50 ml; pH 10.0.

**Table 3 :** Langmuir, Freundlich, D-R and Temkin constants for adsorption of MB by various adsorbents reported in literature.

Adsorbent	$Q_0$ (mg g <sup>-1</sup> )	$b$ (Lmg <sup>-1</sup> )	$k_f$ mg <sup>1-1/n</sup> L <sup>1/ng</sup>	$n$	$q_m$ (molg <sup>-1</sup> )	$E$ kJ/mol	$B$	Référence
Cebia pentandra hull carbon (in the presence of ZnCl <sub>2</sub> activation)	134.5	0.969	81.7	2.14	1596	12.9	10.6	Present study
Gum ghatti/TiO <sub>2</sub>	1305	0.42	916	1.2	918	0.40	68.8	[1]
Citrus limetta peel	227.3	0.02	8.75	1.5	a	a	83.1	[3]
Agar based bimetallic nanoparticles	2272	0.011	18.79	1.07	a	a	107.5	[15]
Sewage sludge+Tea waste	12.5	0.15	8.15	1.0	3.14*10 <sup>-5</sup>	21.82	1782	[17]
Raspberry with TiO <sub>2</sub>	102	0.23	43.3	1.1	97.61	1.47	a	[19]
Γ-Fe <sub>2</sub> O <sub>3</sub> /SiO <sub>2</sub>	26.62	0.15	10.3	5.1	23.9	0.43	a	[22]
NaOH activated chitosan flakes	121.4	a	73.5	8.97	a	a	10.3	[31]

a - Not reported.

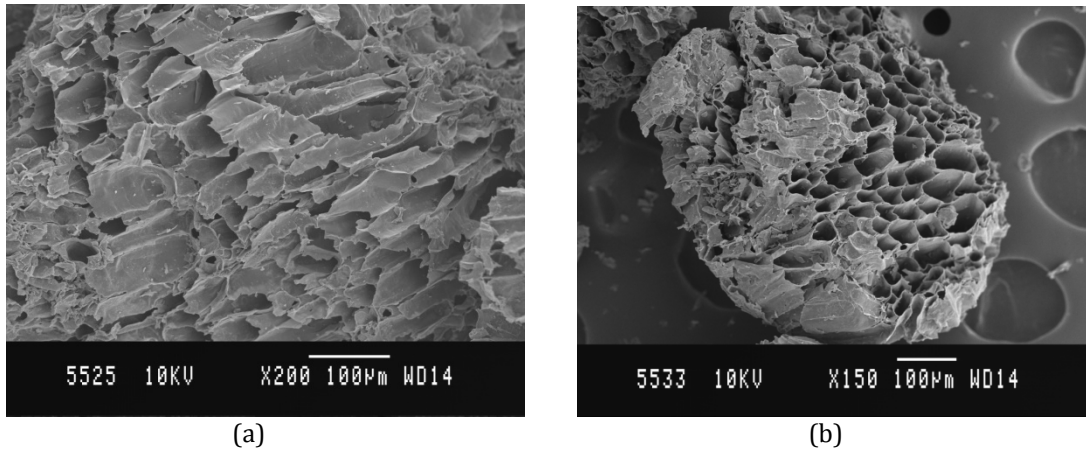


Figure 1 SEM morphology of *Cebia pentandra* a) before and b) after adsorption

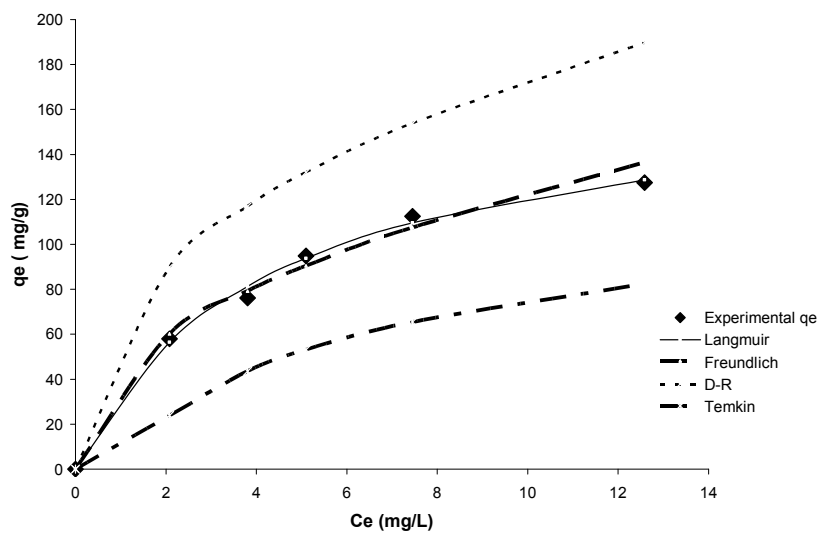


Figure 2 Adsorption isotherms for MB onto ZnCPC

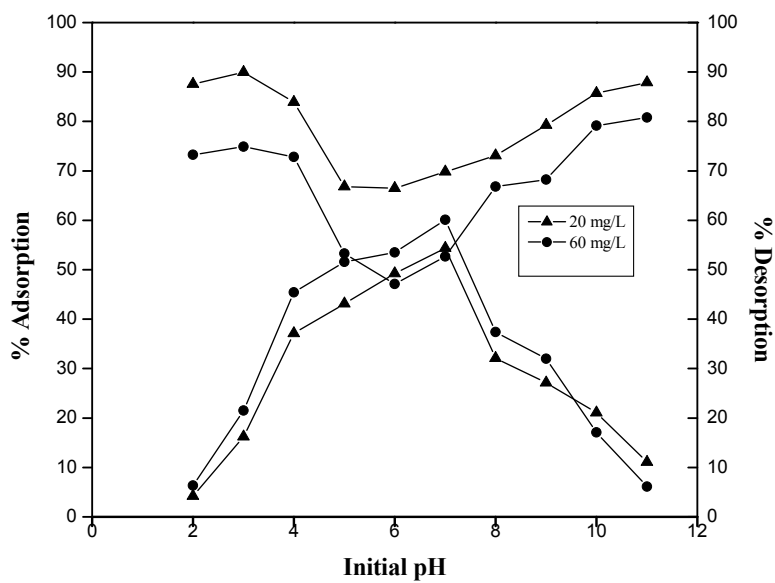


Figure 3 Effect of pH and desorption on MB

## CONCLUSIONS

The present study shows that ZnCl<sub>2</sub> activated carbon developed from an agricultural waste, *Ceiba pentandra*, is an effective adsorbent for the removal of MB from aqueous solution. Equilibrium adsorption data fit better into Langmuir and Freundlich isotherms compared to D-R and Temkin isotherms. Adsorption kinetics followed second order and Banghams model. Langmuir adsorption capacity was found to be 134.5 mg g<sup>-1</sup>. Adsorption was found to be maximum at pH 10.0. pH effect and desorption studies show that physisorption mechanism was involved in adsorption process. Quantitative removal of MB from synthetic wastewater using ZnCPC was also achieved.

## ACKNOWLEDGEMENT

Authors are grateful to the Trustee, Management, Principal and Head of Department of Science & Humanities, Karpagam Institute of technology for their continuous support and providing us lab facilities to carry out the research work.

## REFERENCES

- Mittal H, Sinha Ray S (2016). A study on the adsorption of methylene blue onto gum ghatti/TiO<sub>2</sub> nanoparticles based hydrogel nanocomposite, *Int J Biological Macromolecules*, 88:66-80
- Chang J, Ma J, Ma Q, Zhang D, Qiao N, Hu M, Ma H (2016). Adsorption of methylene blue onto Fe<sub>3</sub>O<sub>4</sub>/activated montmorillonite nanocomposite, *App Clay Science*, 113:132-140.
- Shakoor S, Nasar A (2016). Removal of methylene blue dye from artificially contaminated water using citrus limetta peel waste as a very low cost adsorbent, *J Taiwan Inst of Chemical Eng*, 1:1-10
- Rafatullah M, Sulaiman O, Hashim R, Ahmad A (2010). Adsorption of methylene blue on low cost adsorbents: a review, *J Haz Mat*, 177: 70-80.
- Yan Y, Zhang M, Gong K, Su L, Guo Z, Mao L (2005). Adsorption of methylene blue dye onto carbon nano tubes: a route to an electrochemically functional nano structure and its layer-by-layer assembled nanocomposite, *Chem Mater*, 17: 3457-3463.
- Zhang W, Zhou C, Zhou W, Lei A, Zhang Q, Wan Q (2011). Fast and considerable adsorption of methylene blue dye onto grapheme oxide. *Bull Environ Cont Toxicol*, 87:86-90.
- Bujdak J, Komadel P (1997). Interaction of methylene blue with reduced charge montmorillonite, *J Phy Chem B*, 101: 9065-9068.
- Hassani A, Alidokht L, Khatae A R, Karaca S (2014). Optimization of comparative removal of two structurally different basic dyes using coal as low cost and available adsorbent, *J Taiwan Inst Chem Eng*, 45, 1597-1607.
- Vijayaraghvan K, Mao J, Yun YS (2008). Biosorption of methylene blue from aqueous solution using free and polysulfone-immobilized *Corynebacterium glutamicum* batch and column studies, *Biores Techn*, 99: 2864-2871.
- Njoku VO, Foo K Y, Asif M, Hameed BH (2014). Preparation of activated carbons from rambutan (*Nephelium lappaceum*) peel by microwave-induced KOH activation for acid yellow 17 dye adsorption, *Chem Eng J*, 250:198-204.
- Hai F L, Yamamoto K, Nakajima F, Fukushi K (2012). Application of GAC-coated hollow fibre module for couple enzymatic degradation of dye on membrane to whole cell biodegradation within a membrane bioreactor, *J Membr Sci*, 389:67-75.
- Al-Ahi Y, Li Y (2012). Degradation of C I Reactive blue 19 using combined iron scrap process and coagulation/flocculation by a novel Al (OH)<sub>3</sub>-polyacrylamide hybrid polymer. *J Taiwan Inst Chem Eng*, 43:942-947.
- Gupta N, Kushwala A K, Chattopadhyaya M C (2012). Adsorption studies of cationic dyes onto ashoka leaf power, *J Taiwan Inst Chem Eng*, 43:604-613.
- Sivakumar P, Palaniswamy P N (2009). Adsorption studies of basic red 29 by a non conventional activated carbon prepared from *Euphorbia Antiquorum*, *J Chem Tech Res*, 1: 505-510.
- Patra S, Roy E, Madhuri R, Sharma P K (2016). Agar based bimetallic nanoparticles as high-performance renewable adsorbent for removal and degradation of cationic organic dyes, *J Ind Eng Chem*, 33: 226-238.
- Sana D, Jalila S (2016). Combined effect of unsaturated soil condition and soil heterogeneity on methylene blue adsorption/desorption and transport in fixed bed column: Experimental and modeling analysis, *J King Saud Univ Sci*, 28 : 308-317.
- Fan S, Tang S, Wang Y, Li H, Zhang H, Tang J, Wang Z, Li X (2016). Biochar prepared from co-pyrolysis of municipal sewage sludge and tea waste for adsorption of methylene blue from aqueous solutions: Kinetics, isotherm, thermodynamic and mechanism, *J Molecular Liq*, 220: 432-441.
- Setiabudi H D, Jusoh R, Suhaimi S F R M, Masrur S F (2016). Adsorption of methylene blue onto oil palm leaves : Process optimization , isotherm, kinetics , thermodynamic studies, *J Taiwan Inst of Chem Eng*, 0 : 1-6
- Chen L, Bai B (2013). Equilibrium, kinetic , thermodynamic and insitu regeneration studies about methylene blue adsorption by the raspberry-like TiO<sub>2</sub>@yeast microphores, *Ind Eng Che Res*, 52: 15568-15577.
- Lonappan L, Rouissi T, Das R K, Brar S K, Ramirez A A, Verma M, Surampalli R Y, Valero J R (2016). Adsorption of methylene blue on biochar micro particles derived from different waste materials, *Waste management*, in press
- Duman O, Tunc S, Polat T G, Bozoglan B H (2016). Synthesis of magnetic oxidized multiwalled carbon nanotube-κ-carrageenan-Fe<sub>3</sub>O<sub>4</sub> nanocomposite adsorbent and its application in cationic methylene blue dye adsorption, *Carbohydrate polymers*, 147: 79-88.

22. Chen D, Zeng Z, Zeng Y, Zhang F, Wang M (2016). Removal of methylene blue and mechanism on magnetic  $\gamma$ -Fe<sub>2</sub>O<sub>3</sub>/SiO<sub>2</sub> nano composite from aqueous solution, *Water Res and Ind*, 15:1-13.
23. Gupta V K, Sharma G, Pathania D, Kothiyal N C (2015). Nanocomposite pectin Zr(IV) selenotungstatophosphate for adsorption/photocatalytic remediation of methylene blue and malachite green dyes from aqueous system, *J Ind Eng Chem*, 21:957-964.
24. Molina-Sabio M, Rodriguez-Reinso F (2004). Role of chemical activation in the development of carbon porosity. *Coll Surf A: Physiochem Eng Aspects*, 241: 15-25.
25. Subha R, Namasivayam C (2009). Kinetics and isotherm studies for the adsorption of phenol using low cost micro porous ZnCl<sub>2</sub> activated coir pith carbon. *Can J of Civil Eng*, 8: 1-12.
26. Rengaraj S, Moon S H, Sivabalan R, Arabindoo B, Murugesan V(2002). Removal of phenol from aqueous solution and resin manufacturing industry wastewater using an agricultural waste: rubber seed coat. *J Haz Mat*, B89: 185-196.
27. Zyoud A, Nasar H N I, El-Hamouz A, Hilal S (2015). Soil olive waste in environmental clean up: enhance nitrite ion removed by ZnCl<sub>2</sub> activated carbon, *J Env Mang*, 152 :27-35.
28. Lagergren. S (1898), Zur theorie der sogenannten adsorption geloster stoffe. *Kungliga Sveska Vetenskapskadoemiens Handl*, 24: 1-39.
29. Blanchard G, Maunaye M, Martin G(1984). Removal of heavy metals from water by means of natural zeolite. *Water Res*, 18: 1501-1507.
30. [30] Bhatnagar A, Jain A K (2005). A comparative adsorption studies with different industrial wastes as adsorbents for the removal of cationic dyes from water. *J. Colloid and Interf Sci*, 281: 49-55.
31. Marrakchi F, Ahmed M J, Khanday W A, Asif M, Hameed B H (2017). Mesoporous activated carbon prepared from chitosan flakes by single step sodium hydroxide activation for the adsorption of methylene blue, *Int J Bio Macromole*, 98: 233-239.
32. Langmuir. I (1918). The adsorption of gases on plane surface of glass, mica and platinum , *J Ame. Chem. Soci.*, 40: 1361-1403.
33. Freundlich. H (1906) Uber Die Adsorption in hosungen. *Zeitschrift Fur Physikalische Chemie*, 57: 387-470.
34. Ozcan. A S, Erdem B, Ozcan A (2005). Adsorption of acid blue 913 from aqueous solution onto BTMA –bentonite. *Coll Surf A: Physiochem Engin Aspects*, 266: 73-81.
35. Allen S J, McKay G, Porter J F (2004). Adsorption isotherm models for basic dye adsorption by peat in single and binary component systems. *J. Colloid Interf Sci*, 280: 322-333.
36. Slejko F (1985). *Adsorption Technology a Step by Step Approach to Process Evaluation and Application*, Marcel Decker, New York.
37. Hasany S M, Saeed, M M, Ahmed M (2001). Sorption of traces of silver ions onto polyurethane foam from acidic solution. *Talanta*, 54: 89-98.
38. Wu F C, Tseng R L, Juang R S (2005). Preparation of highly micro porous carbon from fir wood by KOH activation for adsorption of dyes and phenols from water. *Sep. Purif Technol*, 47: 10-19.

#### CITE THIS ARTICLE

R.Subha and D.Anitha. Surface Optimization of nano porous *Ceiba pentandra* hull carbon for the removal of Methylene blue from Aqueous Solution: Kinetics and Isotherms. *Res. J. Chem. Env. Sci.* Vol 5 [4] August 2017. 87-94